Structural Engineering and Mechanics, Vol. 17, No. 3-4 (2004) 467-482
DOI: http://dx.doi.org/10.12989/sem.2004.17.3_4.467

Identification of prestress-loss in PSC beams using modal information

Jeong-Tae Kim†

Smart Structure Engineering Laboratory, Department of Ocean Engineering, Pukyong National University, Busan 608-737, Korea

Chung-Bang Yun‡

Department of Civil and Environmental Engineering, KAIST, Daejon 305-701, Korea

Yeon-Sun Ryu‡ and Hyun-Man Cho‡†

Department of Ocean Engineering, Pukyong National University, Busan 608-737, Korea

(Received February 4, 2003, Accepted November 6, 2003)

Abstract. One of the uncertain damage parameters to jeopardize the safety of existing PSC bridges is the loss of the prestress force. A substantial prestress-loss can lead to severe problems in the serviceability and safety of the PSC bridges. In this paper, a nondestructive method to detect prestress-loss in beam-type PSC bridges using a few natural frequencies is presented. An analytical model is formulated to estimate changes in natural frequencies of the PSC bridges under various prestress forces. Also, an inverse-solution algorithm is proposed to detect the prestress-loss by measuring the changes in natural frequencies. The feasibility of the proposed approach is evaluated using PSC beams for which a few natural frequencies were experimentally measured for a set of prestress-loss cases. Numerical models of two-span continuous PSC beams are also examined to verify that the proposed algorithm works on more complicated cases.

Key words: damage identification; structural safety; prestressed concrete bridge; prestress-loss; modal test; natural frequency.

1. Introduction

This paper deals with the general problem of utilizing dynamic modal properties of structures for nondestructive detection of their damage. Structural damage may be defined as any deviation of a geometric or material property which may cause undesired responses of the structure. A solution to this problem is important for at least two reasons. Firstly, damage detection is the first step in the broader category of safety assessment. Secondly, a timely safety assessment could produce desirable

† Associate Professor
‡ Professor
‡† Post-Doctoral Fellow

consequences such as saving of human lives, protection of property, increased reliability and productivity, and reduction in maintenance costs. Therefore, an accurate and reliable safety assessment capability should be ensured in timely manner to maintain the integrity of structural systems (Stubbs and Osegueda 1990, Pandey *et al*. 1991, Rytter 1993, Kim *et al.* 2003).

In recent years, the interest on the safety assessment of existing prestressed concrete (PSC) bridges has been increased. Prestressed concrete is defined as concrete in which there have been introduced internal stresses of such magnitudes and distribution that the stresses resulting from given external loading are counteracted to a desired degree. The prestress force which is one of unknown parameters in the PSC bridges is introduced to control crack initiation in concrete, to reduce deflections, and to add strength to the prestressed members. Therefore, a substantial difference between the desired and the in-service prestress forces can lead to severe and critical serviceability and safety problems (Saiidi *et al.* 1996, Saiidi *et al.* 1998, Aalami 2000, Miyamoto *et al*. 2000). In other words, a PSC girder is considered as irreparable as it is seriously damaged on the condition of the prestressing strands (Civjan *et al*. 1995). It is known that the loss of the prestress force in tendon occurs due to elastic shortening and bending of concrete, creep and shrinkage of concrete, steel relaxation, anchorage take-up, and frictional loss between tendon and its surrounding materials. Also, the loss of the prestress force unexpectedly occurs due to damage or severing of prestress strands. Therefore, it is very important to estimate the prestress-loss by considering the fact that a prestressed concrete member should keep effective force at each significant level of loading, together with appropriate material properties for that time in the life history of the structure.

Unless a PSC bridge is instrumented at the time of construction, the existing prestress force cannot be directly monitored and other alternative methods should be sought. Based on previous research works, nondestructive evaluation methods using vibration test data can be used to estimate the prestress loss in the PSC bridges on the basis of the following consideration: (1) the loss of the prestress force in the structure is related to the change in structural stiffness (Lin 1963, Saiidi *et al*. 1994); (2) the loss of the prestress force changes vibration characteristics of the structure (Saiidi *et al.* 1994, Miyamoto *et al.* 2000); and (3) the change in structural stiffness can be estimated by monitoring changes in vibration characteristics of the structure (Cawley and Adams 1979, Kim and Stubbs 1995, Stubbs and Kim 1996, Kim and Stubbs 2002, Kim *et al*. 2003). However, to date, no successful attempts have been made to identify the relationship between the prestress-loss and the change in modal parameters (Saiidi *et al*. 1994, Miyamoto *et al*. 2000). Thus, it needs to develop a practical method that can identify the prestress-loss via monitoring changes in natural frequencies. The vibration-based method will prompt the primary, online alarm on the loss of the prestress force before other nondestructive techniques are enforced to diagnosis the state of the structure, in detail.

In this paper, a method to nondestructively detect the loss of prestress force in beam-type PSC bridges using a few natural frequencies is presented. Firstly, an analytical model is described, which has been formulated to identify the relationship between changes in natural frequencies and the loss of prestress force in a PSC beam. Secondly, an inverse-solution algorithm is described, which identifies the prestress-loss in the PSC bridges by using the changes in natural frequencies. Thirdly, the proposed method is applied to a PSC beam, tested by Saiidi *et al.* (1994), for which the lower two natural frequencies are available for a set of prestress-loss cases. Finally, numerical models of two-span continuous PSC beams are examined to verify the practical usability of the proposed algorithm on more complicated cases than the simply-supported PSC beam.

2. PSC beam model

A simply-supported, rectangular, PSC beam with a straight concentric tendon is studied to analyze the effect of the prestress force. As a typical analysis, an axial-force model that represents a beam subject to axial forces is examined. Fig. 1 illustrates an analytic model of a PSC beam for which the prestress force, *N*, is applied at its anchoring edges. For the analysis, the Euler-Bernoulli beam under flexure motion is examined to include effect of compressive loads.

Assuming the axial compression force is uniform along the length of the member and not varying with time, the equation of the free transverse vibration becomes (Clough and Penzien 1993):

$$\frac{\partial^2}{\partial x^2}\left(E_c I_c \frac{\partial^2 y}{\partial x^2}\right) + N\frac{\partial^2 y}{\partial x^2} + \rho_c A_c \frac{\partial^2 y}{\partial t^2} = 0 \tag{1}$$

where y is transverse displacement; $E_c I_c$ is flexural rigidity of concrete beam-section; and $\rho_c A_c$ is mass of concrete beam per unit length. Eq. (1) with the boundary conditions leads to the nth natural frequency as follows:

$$\omega_n^2 = \left(\frac{n\pi}{L}\right)^4 \frac{E_c I_c}{\rho_c A_c} - \left(\frac{n\pi}{L}\right)^2 \frac{N}{\rho_c A_c} \tag{2}$$

Eq. (2) shows that the increase in the axial compression reduces the frequency and vise versa. However, this is contradictory to the behavior of the PSC beam with straight concentric tendons since natural frequencies are reduced as a result of the loss of prestress force (Saiidi *et al*. 1994).

As an alternative analysis, a tension-strength model is examined for the PSC beam with straight concentric tendons. Fig. 2 schematizes the tension-strength model for which a tendon is initially stretched and anchored to introduce prestressing effect. Suppose that the structure is in axial compression due to the prestress loads applied at the anchorage edges. Then we can model the structure which is initially deformed in compression (e.g., up to the deformed span length L_r) and

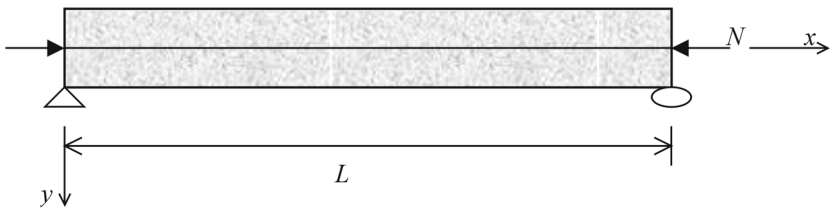

(a) PSC beam under axial-force

(b) Euler-Bernoulli beam under axial-force

Fig. 1 Axial-force model of PSC beam

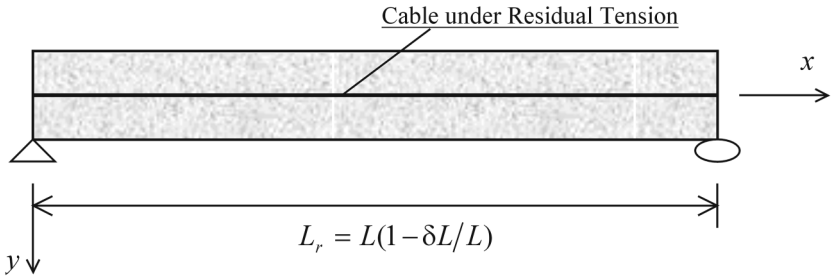

(a) PSC beam under initial deformation

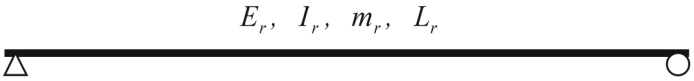

(b) Beam of equivalent flexural rigidity

Fig. 2 Tension-strength model of PSC beam

the tendon is still in tension due to the constraint after elastic stretching for prestressing effect. The initial deformation of the beam results in the reduction of span length, $\delta L(= L - L_r)$, and the expansion in the cross-section by Poisson effect. The governing differential equation for the beam is expressed by:

$$\frac{\partial^2}{\partial x^2}\left(E_r I_r \frac{\partial^2 y}{\partial x^2}\right) + m_r \frac{\partial^2 y}{\partial t^2} = 0 \tag{3}$$

where $E_r I_r$ is the flexural rigidity of PSC beam section and m_r is mass per unit length of PSC beam. The composite flexural rigidity and the mass of the PSC beam can be evaluated as:

$$E_r I_r = E_c I_c + E_s I_s \tag{4a}$$

$$m_r = \rho_c A_c + \rho_s A_s \tag{4b}$$

where $E_s I_s$ is the equivalent flexural rigidity corresponding to the contribution of the tendon on the flexural resistance and $\rho_s A_s$ is the mass of the tendon per unit length.

The equivalent flexural rigidity, $E_s I_s$, is derived from analyzing flexural vibration of a cable under uniform tension as shown in Fig. 3(a). The governing differential equation of the cable for tension force N is given by (Clough and Penzien 1993):

$$-N\frac{\partial^2 y}{\partial x^2} + \rho_s A_s \frac{\partial^2 y}{\partial t^2} = 0 \tag{5}$$

Furthermore, Eq. (5) leads the nth natural frequency of the cable under tension as follows (see Fig. 3(a)):

$$\omega_n^{c2} = \left(\frac{n\pi}{L_r}\right)^2 \frac{N}{\rho_s A_s} \tag{6}$$

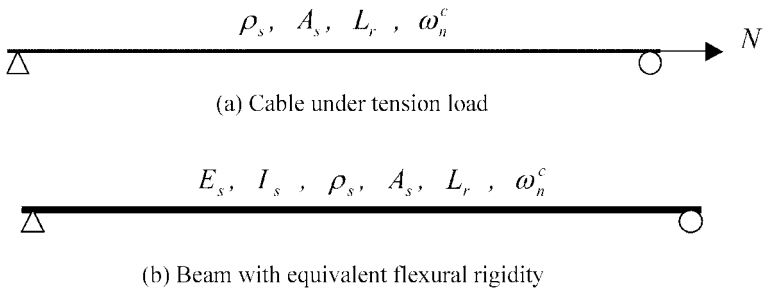

(a) Cable under tension load

(b) Beam with equivalent flexural rigidity

Fig. 3 Flexural vibration of cable under tension

On assuming that there exists a beam equivalent to the cable under tension with respect to modal properties, as shown in Fig. 3(b), the *n*th natural frequency of the equivalent beam is derived as follows:

$$\omega_n^{c2} = \left(\frac{n\pi}{L_r}\right)^4 \frac{E_s I_s}{\rho_s A_s} \tag{7}$$

By setting Eq. (6) equal to Eq. (7), we obtain the equivalent flexural rigidity as follows:

$$E_s I_s = \left(\frac{L_r}{n\pi}\right)^2 N \tag{8}$$

On substituting Eq. (8) into Eq. (4), the total flexural rigidity of the PSC beam section can be expressed as:

$$E_r I_r = E_c I_c + \left(\frac{L_r}{n\pi}\right)^2 N \tag{9}$$

where $E_r I_r$ is assumed constant along the entire length of the beam.
Applying Eq. (9) and appropriate boundary conditions to Eq. (3) leads the *n*th natural frequency of the residual-tension model as follows:

$$\omega_n^2 = \left(\frac{n\pi}{L_r}\right)^4 \frac{1}{m_r}\left(E_c I_c + \left(\frac{L_r}{n\pi}\right)^2 N\right) \tag{10}$$

where the deformed span length L_r can be computed as:

$$L_r = L\left(1 - \frac{\delta L}{L}\right) = L\left(1 - \frac{N}{A_c E_c}\right) \tag{11}$$

In case of $A_c/L^2 << 1$, the axial compression effect is negligible if the prestress force N is less than the beam's yielding point. Note that the residual tension effect of the tendon is reflected on the natural frequency equation of the PSC beam via quantifying the equivalent bending rigidity which is in terms of the beam span length and the axial force. Note also that Eq. (10) can be directly used to compute frequency changes due to changes in prestress forces.

As an inverse solution of Eq. (10), the prestress force can be identified as:

$$(N)_n = \omega_n^2 m_r \left(\frac{L_r}{n\pi}\right)^2 - E_c I_c \left(\frac{n\pi}{L_r}\right)^2 \tag{12}$$

where $(N)_n$ is the identified prestress force by using nth natural frequency and structural properties. By assuming that no changes in beam's geometry and material properties occur due to changes in the prestress force, the first variation of the prestress force can be derived as:

$$(\delta N)_n = \delta\omega_n^2 m_r \left(\frac{L_r}{n\pi}\right)^2 \tag{13}$$

where $(\delta N)_n$ is the change in the prestress force that can be identified by the nth mode and $\delta\omega_n^2$ is the change in ω_n^2 due to the prestress-loss. From Eq. (12) and Eq. (13), the relative change in the prestress force that can be identified by using the nth mode is obtained as:

$$\left(\frac{\delta N}{N}\right)_n = \frac{\delta\omega_n^2 m_r \left(\frac{L_r}{n\pi}\right)^2}{\omega_n^2 m_r \left(\frac{L_r}{n\pi}\right)^2 - E_c I_c \left(\frac{n\pi}{L_r}\right)^2} \tag{14}$$

Rearranging Eq. (14) gives:

$$\left(\frac{\delta N}{N}\right)_n = \frac{\delta\omega_n^2}{\omega_n^2 - \varpi_n^2} \tag{15}$$

where ϖ_n^2 is the nth natural frequency of the beam with zero prestress force and is given by:

$$\varpi_n^2 = \left(\frac{n\pi}{L_r}\right)^4 \frac{E_c I_c}{m_r} \tag{16}$$

From Eq. (15), the relative change in prestress force, $\delta N/N$, can be estimated by measuring natural frequency changes, $\delta\omega_n$, and natural frequencies of the beam with zero prestress force, ϖ_n. However, in existing real structures, ϖ_n is not available unless measured at as-built state; therefore, ϖ_n should be estimated from system identification process.

3. Verification examples

3.1 Example 1: Simply-supported PSC beam

3.1.1 Description of test structure

The test structure is schematized in Fig. 4. Saiidi *et al.* (1994) performed a laboratory experiment to measure changes in dynamic modal properties by adjusting prestress forces applied to the test structure. The beam was reinforced longitudinally and transverse direction with Grade 60 bars. The stirrups were used to facilitate the positioning of the top bars. A Grade 250 seven-wire straight concentric strand was used as the prestressing steel. The strand was placed in a 25-mm diameter duct that remained ungrouted. The concrete was made with type II Portland cement and had a maximum aggregate size of 12.7-mm. The 28-day compressive strength of concrete was 20.3 MPa.

Dynamic modal tests were conducted with different axial forces. For the modal tests, the beam was instrumented with seven equally spaced accelerometers that measured the vertical acceleration responses of the beam. The structure was excited by impact hammer in vertical direction. Each dynamic test was performed after the desired prestress force had been applied and the cable had been anchored. The jack was disconnected from the beam to avoid the effect of the jack mass on

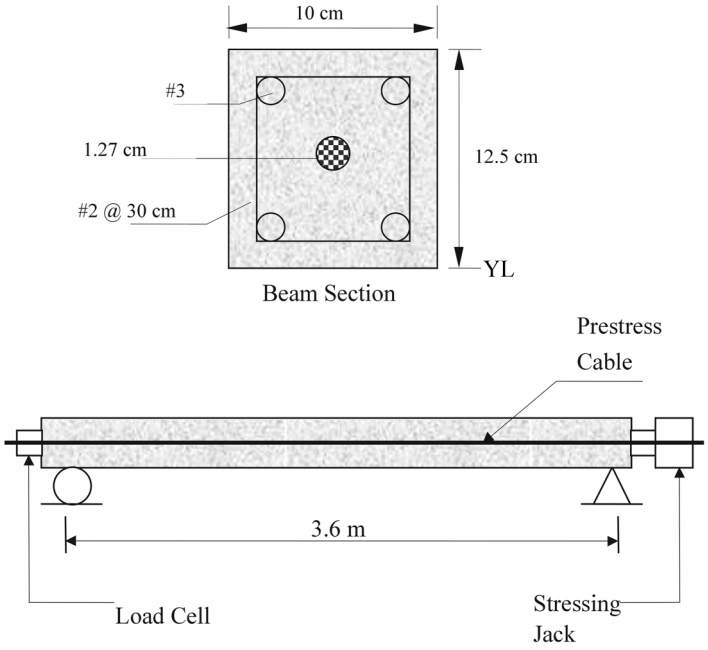

Fig. 4 Simply-supported PSC beam (Saiidi *et al.* 1994)

Table 1 Natural frequencies of simply-supported PSC beams

Case	In-situ prestress force (kN)	Experimental frequency (Hz) (Saiidi *et al.* 1994)		Predicted frequency (Hz)			
				Analytical model		FE model	
		Mode 1	Mode 2	Mode 1	Mode 2	Mode 1	Mode 2
1	0	11.41	43.99	11.409	45.635	11.196	44.047
2	15.71	12.09	44.11	11.832	46.063	11.689	44.547
3	27.05	13.47	44.89	12.128	46.371	12.032	44.886
4	36.49	12.89	44.69	12.370	46.626	12.311	45.161
5	57.25	13.63	45.62	12.885	47.179	12.902	45.744
6	81.81	14.49	45.57	13.468	47.828	13.568	46.401
7	91.26	14.72	46.32	13.686	48.073	13.816	46.645
8	121.46	14.72	45.86	14.360	48.854	14.578	47.398
9	130.91	14.97	46.10	14.565	49.096	14.809	47.622
10	132.80	15.07	45.87	14.610	49.145	14.855	47.667

the beam's dynamic responses. The prestress force was varied from zero to a relatively large level, i.e., the maximum axial force was 131.3 kN.

Four sets of modal data were collected for each axial force level, two with impact applied at mid-span and the other two with impact at the quarter point. Using fast Fourier transformation technique (FFT), the first two frequencies were obtained for each in-situ prestress-force case as listed in Table 1. The listed frequencies are the average values of the results measured at all seven channels.

3.1.2 System identification

The natural frequencies of the PSC beam in Fig. 4 were identified by using two different models: analytical and FE models. The analytical model is equivalent to Eq. (10) from which natural frequencies are directly computed for known prestress forces. The span length L_r is approximated using Eq. (11). The elastic modulus of concrete was estimated as E_c = 21.52 GPa by using the 28-day compressive strength f_{28} = 20.3 MPa, the linear mass density of concrete ρ_c = 2400 kg/m^3, and cross-sectional area of concrete $A_c = 1.24 \times 10^{-2}$ m^2. For the maximum force (i.e., N = 132.8 kN) in Table 1, L_r is computed as 0.9995 L, i.e., the resulting compressive strain is less than 5×10^{-4}. Therefore, we neglect the axial deformation effect provided that $L_r \approx L (= 3.6\ \text{m})$. Also, the second moment of area is calculated as $I_c = 1.734 \times 10^{-5}$ m^4. The mass per unit length are calculated using Eq. (4b) as m_r = 30.75 kg/m, in which the cross-sectional area and the linear mass density of the steel tendon are $A_s = 1.27 \times 10^{-4}$ m^2 and ρ_s = 7850 kg/m^3, respectively.

With the above structural data, Eq. (10) can be rewritten and regarded as an analytical model to predict natural frequencies of the PSC beam.

$$\omega_n^2 = 5133.3 \times n^4 + 0.0247 n^2 N \tag{17}$$

where n is mode number and N is the prestress force in Newton. Here all ten cases in Table 1 were investigated by using Eq. (17). The predicted natural frequency results are also summarized in Table 1.

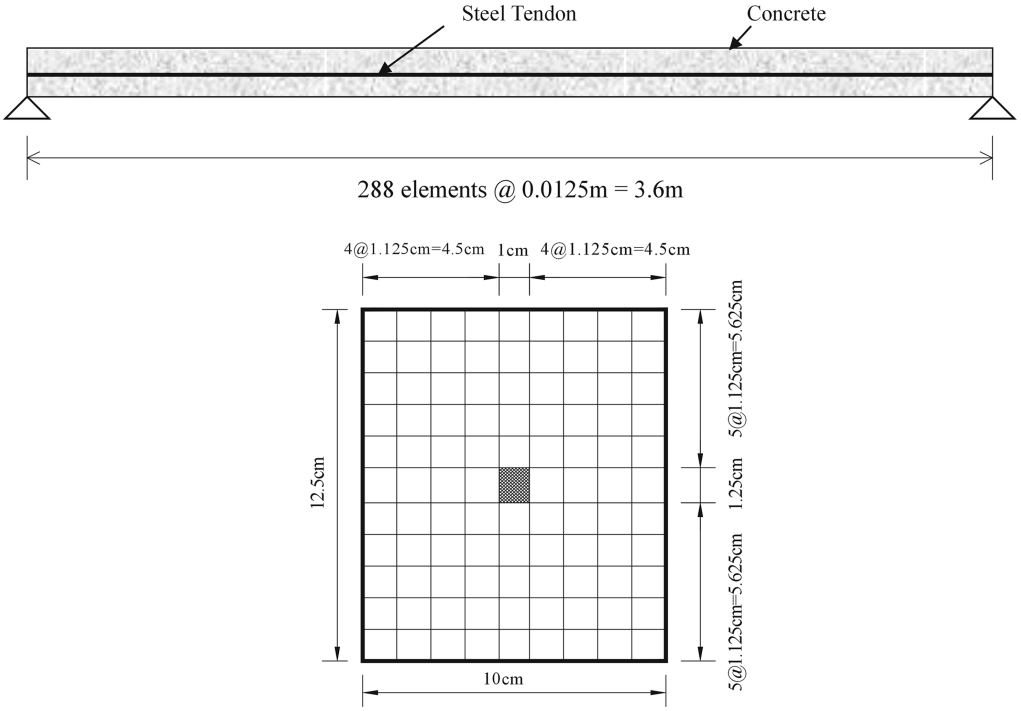

Fig. 5 FE model of simply-supported PSC beam

The FE model of the PSC beam is schematized in Fig. 5. For analysis purpose, we divided the beam into 28,512 block elements. The steel tendon is placed at center with 288 elements along the beam and each element size is 1 cm × 1.25 cm × 1.25 cm. All others are concrete elements and each element size is 1.125 cm × 1.125 cm × 1.25 cm. Material properties of the FE model were assigned as follows: (1) for concrete elements, the elastic modulus E_c = 21.52 GPa, Poisson's ratio υ = 0.18, and the linear mass density ρ_c = 2400 kg/m^3; and (2) for steel tendon elements, $E_s = 0.3155 \cdot \mathrm{N} \cdot \mathrm{n}^{-2}$ (kN/m^3), ρ_s = 7850 kg/m^3, and υ = 0.3. Among those properties, the elastic modulus E_s is estimated by using the equivalent flexural rigidity formula.

$$E_s = \frac{L^2 N}{n^2 \pi^2 I_s} = 0.3155 \frac{N}{n^2} (\mathrm{kN/m^2}) \tag{18}$$

where I_s is the second moment of area of the steel tendon element and $I_s = 4.16 \times 10^{-3}$ m^2. Since the modal and structural properties depends on mode number (see Eq. (6) and Eq. (7)), E_s is estimated differently for each mode. Therefore, E_s should be adjusted for each mode. For example, $E_s = 0.3155 \cdot N$ (kN/m^2) for the first bending mode and $E_s = 0.0789 \cdot N$ (kN/m^2) for the second one. The contribution of the tendon to the flexural stiffness becomes the maximum in the first bending mode and decreases as mode number increases. Modal parameters of the FE model were generated numerically using the commercial software ANSYS. Here all ten cases in Table 1 were investigated. The predicted frequencies of modes 1 and 2 are also summarized in Table 1. Their mode shapes are respectively plotted in Fig. 6.

The predicted frequencies using those two models were compared with the experimentally measured ones as plotted in Figs. 7(a) and 7(b). In case of the analytical model, prediction errors are 0.1%~3% for mode 1 and 3%~7% for mode 2. In case of the FE model, prediction errors are 1%~3% for mode 1 and 0.1%~4% for mode 2. In mode 1, the predicted results show relatively good accuracy in both models. In mode 2, the results of the FE model shows relatively better accuracy than the analytical model.

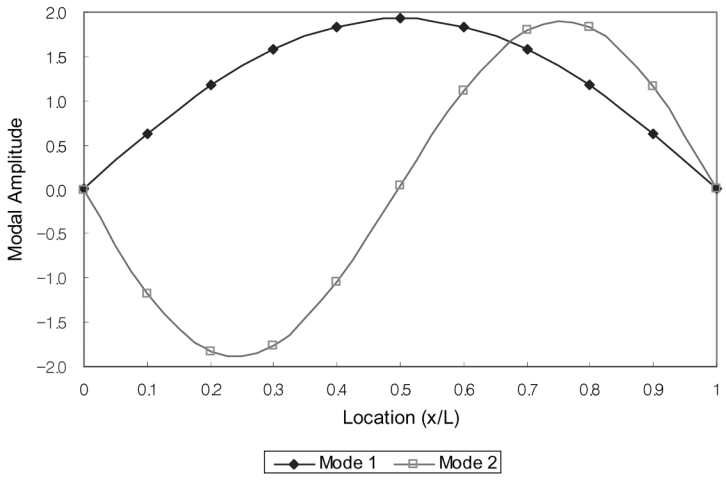

Fig. 6 Mode shapes of simply-supported PSC beam

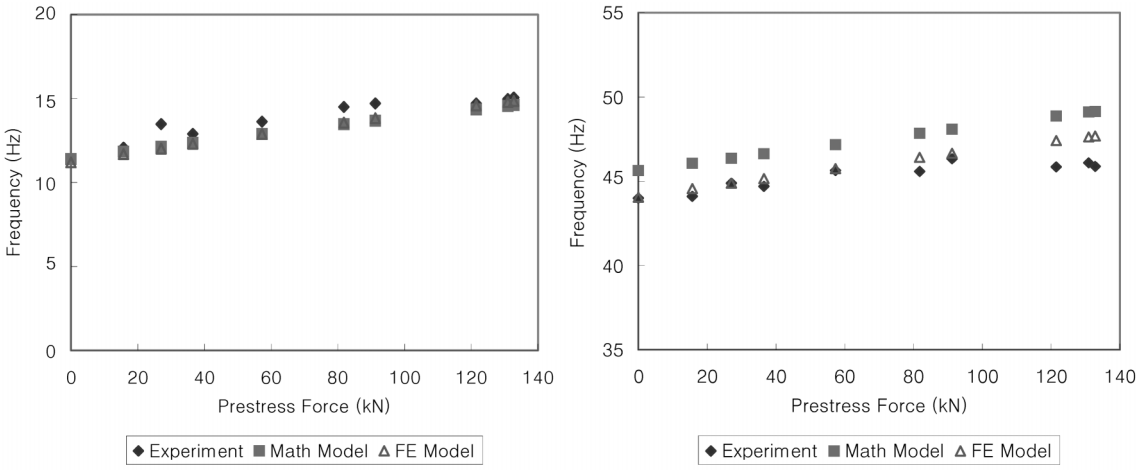

(a) Mode 1 (b) Mode 2

Fig. 7 Natural frequencies of simply-supported PSC beam

3.1.3 Prestress-loss detection

The prestress-loss in the test structure is identified from the inverse solution of the PSC beam models. The relative change in prestress force with reference to the full prestress force is identified by measuring the relative change in the *n*th natural frequency with reference to the frequency margin between the full prestress state and the zero prestress state. In order to predict the prestress-losses for the cases in Table 1, Eq. (15) is rewritten as follows:

$$\frac{\delta N}{N_f} = \frac{\delta \omega_n^2}{\omega_{nf}^2 - \varpi_n^2} = \frac{\omega_{nf}^2 - \omega_{nd}^2}{\omega_{nf}^2 - \varpi_n^2} \tag{19}$$

where the subscripts f and d denote the full prestress state and the damaged prestress-loss state, respectively. In real structures, natural frequencies can be measured at those two states. However, natural frequencies of the zero prestress state (ϖ_n) should be estimated, since it is not realistic to measure the frequencies in existing in-service structures. In this study, ϖ_n is modeled by the analytical model for $N = 0$ (i.e., 11.409 Hz for mode 1 and 45.635 Hz for mode 2) and also by the FE model for $N = 0$ (i.e., 11.196 Hz for mode 1 and 44.047 Hz for mode 2). Here all ten cases in Table 1 were examined to detect the prestress-loss and the results are outlined in Table 2.

The predicted prestress-losses using the two models were compared with the measured in-situ prestress-losses. The predicted prestress-losses versus the inflicted prestress-losses were plotted in Fig. 8. The correlation between those two sets is relatively high both in the FE model and in the analytical model. It means that the prestress-loss in the PSC beam can be detected via monitoring changes in natural frequencies of a few basic modes. In case of the analytical model, prediction errors are 1%~72% for mode 1 and even higher for mode 2. In case of the FE model, prediction errors are 5%~75% for mode 1 and 10%~70% for mode 2. It is observed that the accuracy of the predicted prestress-loss depends on the accuracy of measured frequencies and the accuracy of the baseline modeling of the zero force state as well. In mode 1, both models show almost identical results. In mode 2, the FE model shows relatively better accuracy than the analytical model.

Table 2 Prestress-loss prediction in simply-supported PSC beams

Case	Experiment		Analytical model		FE model	
	N (kN)	$\partial N/N$	$(\partial N/N)_1$	$(\partial N/N)_2$	$(\partial N/N)_1$	$(\partial N/N)_2$
1	0	1.0	0.999	-	0.953	-
2	15.71	0.882	0.835	-	0.795	0.994
3	27.05	0.796	0.471	-	0.449	0.559
4	36.49	0.725	0.629	-	0.599	0.671
5	57.25	0.569	0.426	-	0.406	0.144
6	81.81	0.384	0.177	-	0.169	0.172
7	91.26	0.313	0.108	–1.930	0.103	–0.261
8	121.46	0.085	0.108	0.043	0.103	0.006
9	130.91	0.014	0.031	–0.934	0.029	–0.133
10	132.80	0.0	0.0	0.0	0.0	0.0

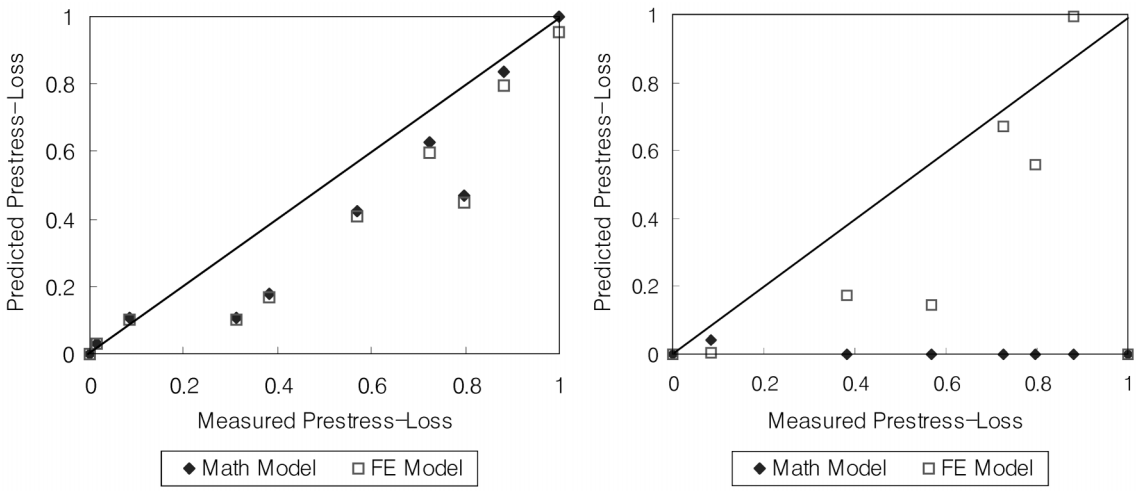

(a) Mode 1 (b) Mode 2

Fig. 8 Prestress-loss prediction in simply-supported PSC beam

In reality, the elastic modulus of concrete varies with time, which would also cause change in frequency. The proposed method alone may not be able to distinguish or isolate the change in prestress-loss from the concrete damage based on the frequency shift. However, a frequency-based algorithm or a mode-shape-based algorithm proposed by the authors (Kim *et al*. 2003, Kim and Stubbs 2002) could be applied in conjunction with the proposed method to identify the location and the severity of damage in the concrete beam.

3.2 Example 2: Two-span continuous PSC beam

Numerical models of two-span continuous PSC beams are examined to verify the practical usability of the proposed algorithm on more complicated cases than the simply-supported PSC

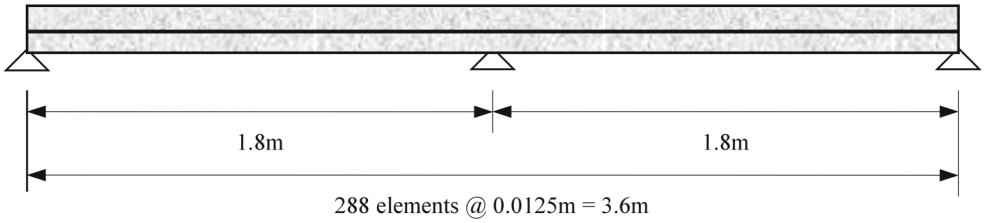

(a) Periodic beam

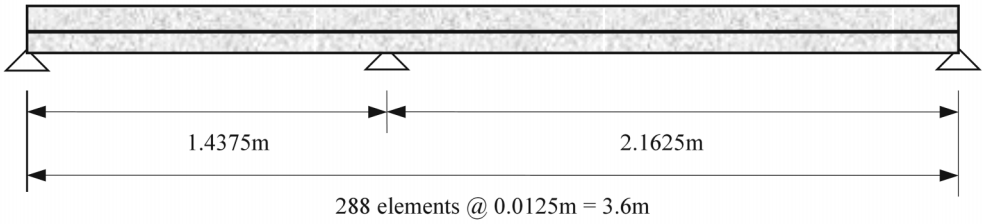

(b) Non-periodic beam

Fig. 9 Two-span continuous PSC beams

beam. In Fig. 9, a periodic beam (the left span to the right span is *0.5L:0.5L*) and a non-periodic beam (the left span to the right span is *0.4L:0.6L*) are shown. For both cases, the boundary conditions are set as hinged, roller, and roller supports from the left. The FE models of the beams have the same beam geometry as the simply-supported beam, which is shown in Fig. 5. For analysis purpose, we divided each beam into 28,512 block elements. The steel tendon is placed at center with 288 elements (the same as Example 1). Material properties of the FE models were also the same as the Example 1.

Modal parameters of the FE models were generated using the ANSYS software. All ten cases of the prestress forces listed in Table 1 were again investigated. The equivalent flexural rigidity formula was used for simulating the prestress forces. Here, Eq. (18) was used to compute the equivalent flexural rigidity E_sI_s. Using only mode 1, $E_s = 0.3155 \cdot N$ (kN/m^2) and $I_s = 4.16 \times 10^{-3}$ m^2. For the two beams shown in Fig. 9, natural frequencies of the first two bending modes were computed and listed in Table 3. Mode shapes of the first two bending modes are also plotted in Fig. 10.

Next, the prestress-losses of the PSC beams are predicted by using Eq. (19). The relative change in the *n*th natural frequency is measured with reference to the frequency margin between the full prestress state and the zero prestress state. For those two beams, all ten cases of the prestress forces were examined and the prestress-loss prediction results are outlined in Table 4. The results of both periodic and non-periodic beams are shown there, respectively. Also, the predicted prestress-losses versus the simulated prestress-losses were plotted in Fig. 11. As shown in Fig. 11(a), in the periodic beam, the predicted prestress-losses are almost identical to the simulated ones. Also, as shown in Fig. 11(b), in the non-periodic beam, the correlation between the simulated prestress-loss and the predicted one is reasonably high. It means that the prestress-loss in the two-span PSC beams could be detected via monitoring the changes in natural frequencies of a few basic modes. The results are almost identical for both mode 1 and mode 2.

Table 3 Natural frequencies of two-span continuous PSC beams

Case	Prestress force (kN)	Natural frequency (Hz)			
		Periodic beam		Non-periodic beam	
		Mode 1	Mode 2	Mode 1	Mode 2
1	0	44.060	67.435	38.150	80.657
2	15.71	46.034	70.595	38.730	84.477
3	27.05	47.388	72.685	39.115	86.680
4	36.49	48.488	74.377	39.421	88.441
5	57.25	50.821	77.955	40.054	92.115
6	81.81	53.444	81.964	40.749	96.152
7	91.26	54.419	83.451	41.004	97.625
8	121.46	57.420	88.013	41.781	102.06
9	130.91	58.327	89.389	42.014	103.38
10	132.80	58.506	89.660	42.060	103.63

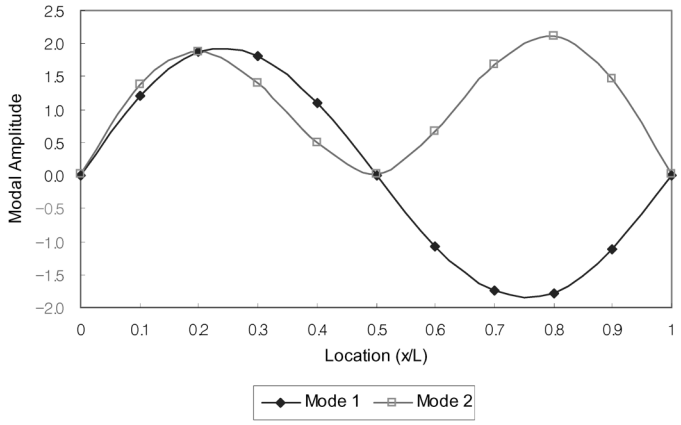

(a) Periodic beam

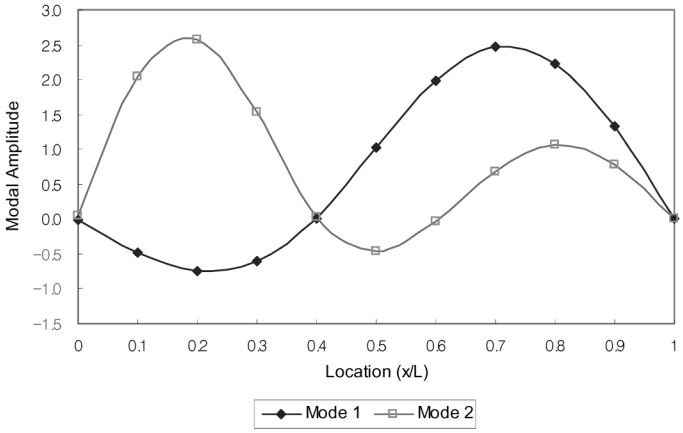

(b) Non-periodic beam

Fig. 10 Mode shapes of simply-supported PSC beam

Table 4 Prestress-loss prediction in two-span continuous PSC beams

Case	Simulation		Periodic beam		Non-periodic beam	
	N (kN)	$\partial N/N$	$(\partial N/N)_1$	$(\partial N/N)_2$	$(\partial N/N)_1$	$(\partial N/N)_2$
1	0	1.0	1.0	1.0	1.0	1.0
2	15.71	0.882	0.879	0.875	0.858	0.851
3	27.05	0.796	0.795	0.789	0.762	0.762
4	36.49	0.725	0.723	0.718	0.686	0.673
5	57.25	0.569	0.567	0.562	0.525	0.532
6	81.81	0.384	0.383	0.378	0.346	0.353
7	91.26	0.313	0.312	0.308	0.279	0.286
8	121.46	0.085	0.085	0.084	0.075	0.076
9	130.91	0.014	0.014	0.014	0.012	0.012
10	132.80	0.0	0.0	0.0	0.0	0.0

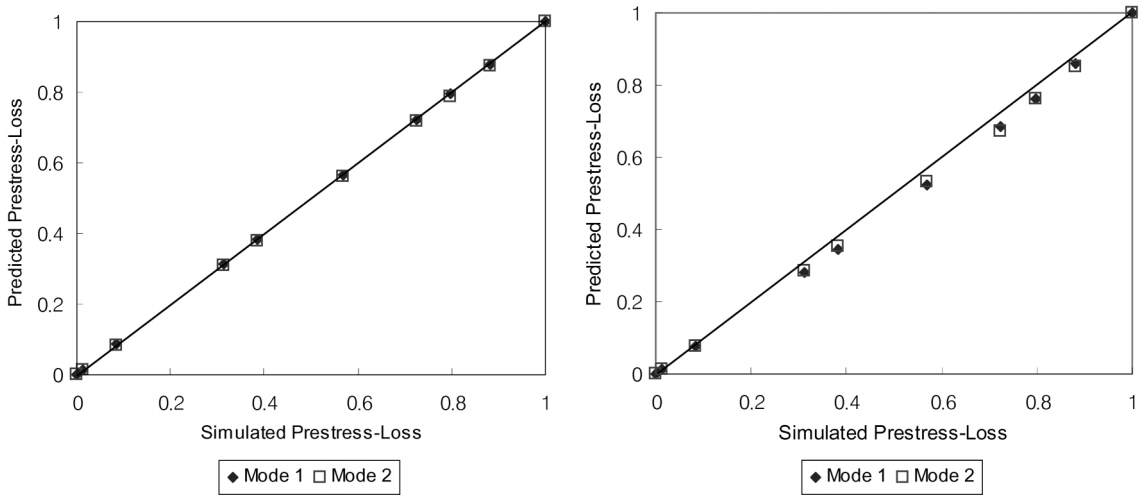

(a) Periodic beam (b) Non-periodic beam

Fig. 11 Prestress-loss prediction in 2-span continuous PSC beams

4. Conclusions

A methodology to nondestructively detect prestress-loss in beam-type PSC bridges using a few natural frequencies was presented. An analytical model to estimate natural frequencies of the PSC bridges under various prestress forces was developed. Also, an inverse-solution algorithm to predict prestress-loss was formulated. The feasibility and practicality of the model was evaluated and verified using PSC beams for which a few natural frequencies were measured for a set of prestress-loss cases. Finally, numerical models of two-span continuous PSC beams were also examined to verify the practical applicability of the proposed algorithm on more complicated cases.

For the application of the proposed approach to the test structure, natural frequencies were predicted by using the analytical model whereas prestress-losses were predicted by using the inverse-solution algorithm. The natural frequencies predicted at several prestressing stages showed relatively accurate results compared to the ones measured at the same stages. It was also observed that both in FE model and analytical model, the correlation between the inflicted and the predicted prestress-losses was relatively high. Hence, the prestress-loss in the PSC beam can be detected via monitoring the changes in natural frequencies of a few basic modes. Future research needs are to improve the accuracy of prestress-loss prediction, to distinguish the change in prestress-loss from the concrete damage based on the frequency shift, and to improve the accuracy of baseline modeling of the initial zero-force state of the structure.

Acknowledgements

This work was supported by Smart Infra-Structure Technology Center and KOSEF in the program years of 2002-2003. The authors would like to express their sincere appreciation to Prof. Norris Stubbs at Texas A&M University for providing his research facilities to this paper.

References

Aalami, B.O. (2000). "Structural modeling of posttentioned members", *J. Struct. Eng.*, ASCE, **126**(2), 157-162.

Cawley, P. and Adams, R.D. (1979), "The location of defects in structures from measurements of natural frequencies", *J. Strain Analysis*, **14**(2), 49-57.

Clough, R.W. and Penzien, J. (1993), *Dynamic of Structures*, McGraw Hill, USA.

Civjan, S.A., Jirsa, J.O., Carrrasquillo, R.L. and Fowler, D.W. (1995), "Method to evaluate remaining prestress in damaged prestressed bridge girders", Research Report 1370-2, Center for Transportation Research, University of Texas at Austin.

Kim, J.T. and Stubbs, N. (1995), "Model-uncertainty impact and damage-detection accuracy in plate girder", *J. Struct. Eng.*, ASCE, **121**(10), 1409-1417.

Kim, J.T. and Stubbs, N. (2002), "Improved damage identification method based on modal information", *J. Sound Vib.*, **252**(2), 223-238.

Kim, J.T., Ryu, Y.S., Cho, H.M. and Stubbs, N. (2003), "Damage identification in beam-type structures: frequency-based method vs mode-shape-based method", *Eng. Struct.*, **25**, 57-67.

Lin, T.Y. (1963), *Design of Prestressed Concrete Structures*, John Wiley & Sons, USA.

Miyamoto, A., Tei, K., Nakamura, H. and Bull, J.W. (2000), "Behavior of prestressed beam strengthed with external tendons", *J. Struct. Eng.*, ASCE, **126**(9), 1033-1044.

Pandey, A.K., Biswas, M. and Samman, M.M. (1991), "Damage detection from changes in curvature mode shapes", *J. Sound Vib.*, **145**(2), 321-332.

Rytter, A. (1993), "Vibration based inspection of civil engineering", Ph.D. Dissertation, University of Aalborg, Denmark.

Saiidi, M., Douglas, B. and Feng, S. (1994), "Prestress force effect on vibration frequency of concrete bridges", *J. Struct. Eng.*, ASCE, **120**(7), 2233-2241.

Saiidi, M., Shield, J., O'Connor, D. and Hutchens, E. (1996), "Variation of prestress force in a prestressed concrete bridge during the first 30 months", *PCI Journal*, **41**(5), 66-72.

Saiidi, M., Hutchens, E. and Gardella, D. (1998), "Bridge prestress losses in dry climate", *Journal of Bridge Engineering*, ASCE, **3**(3), 111-116.

Stubbs, N. and Osegueda, R. (1990), "Global nondestructive damage evaluation in solids", *Int. J. Analytical and Experimental Modal Analysis*, **5**(2), 67-79.
Stubbs, N. and Kim, J.T. (1996), "Damage localization in structures without baseline modal parameters", *AIAA Journal*, **34**(8), 1649-1644.